Journal of Renewable Materials
DOI:10.32604/jrm.2020.09575
Article

Tech Science Press

Mechanical Behavior of Light Trusses Made of Poplar Laminated Veneer Lumber and Connected with Bolts and Tooth Plates

Yan Liu[1], Yanfei Guo[1], Xufeng Sun[1,*] and Meng Gong[2]

[1]College of Civil Engineering, Yangzhou University, Yangzhou, China
[2]Wood Science and Technology Center, University of New Brunswick, Fredericton, Canada
*Corresponding Author: Xufeng Sun. Email: xfsun@yzu.edu.cn
Received: 20 December 2019; Accepted: 18 May 2020

Abstract: Poplar Laminated Veneer Lumber (Poplar LVL) is a new type of engineering materials with high strength, good reliability and small variability. Poplar LVL is manufactured from the fast-growing poplar, which is widely used in packaging, furniture and others, however, is rarely adopted in construction. In order to explore the feasibility of poplar LVL trusses in construction of roof, four 4.5-m-span Fink-and-Howe trusses were designed and assembled, which were made of poplar LVL with bolted- and tooth-plated connections. Vertical static loading on the upper chord joints of a truss was imposed by self-balancing test device. The mechanical properties of trusses were examined. The ultimate load, deformation character and failure mode of each truss were measured, observed and analyzed. Furthermore, four types of analytical models with different joint connection assumptions were used to estimate the ultimate load and deflection. The results showed that the poplar LVL trusses were basically in elastic stage before the design load was reached, showing good working performance under the action of design load. The bearing capacity of the trusses of bolted connections was greater than that of the tooth-plated connections. As for the same joint connection type, the bearing capacity of Fink trusses exceeded that of Howe trusses. The poplar LVL light trusses of both types of connections showed good structural performance, which could be reasonably used for building roof systems.

Keywords: Poplar LVL; truss; mechanical properties; bearing capacity; bolted connection; truss plate connections; model

1 Introduction

The Chinese government has been recently encouraging the development of bamboo and wood buildings in accordance with local conditions. Many studies developed various types of connections for original bamboo structures such as welded joints [1–3]. Due to the shortage of forest resources in China, the research on the mechanical properties of adhesively laminated wood products was conducted, which were made of the wood from the fast-growing forests. Among them, poplar laminated veneer lumber (poplar LVL), made of fast-growing poplar trees, shows many advantages such as high strength, good

reliability and small variability. Thus, poplar LVL has been widely used in packaging, furniture and other, however, it is seldom used in construction such as roof systems in a building.

There are many studies on light wood trusses with different connection methods, different species and different truss types [4–8]. Matteo Barbari et al. [9] introduced a new connection system for traditional timber trusses and conducted the finite element analysis (FEA) on their bearing capacities, discovering that the bearing capacity of the developed connection systems was 4 time higher than the design value. Xu et al. [10] studied the stress state and failure mode of light trusses made of imported dimension lumber and tooth plates. On the basis of Johnson's yield theory, Beineke et al. [11] put forward a kind of "linear model" of calculating the bearing capacity of the light wood trusses based on the "plate-tooth independent model" and "plate-tooth continuous model." Misra [12] examined the stress distribution of punched metal plates in timber joints, indicating that the stresses around a metal plate were not uniform. Foschi [13] published nonlinear analysis of a metal plate connected wood truss joints considering several factors which were used to determine its effect on the truss deformation and ultimate load of a plated connection. Toan [14] conducted a study of testing the tension joints in four-way plating setups and concluded that the axial and shear forces were, by assuming a rigid connection, uniformly distributed, suggesting the calculation of this type of tension joints was very conservative. Maraghechi et al. [15] developed a matrix analysis method for a plane-framed structure with nonrigid connections. They found that a good correlation could be obtained by comparing tests of two frames and several beams with analytical results. Lum et al. [16] reported, after testing a 12.2 m parallel roof truss and comparing the results from the SAT program and standard plane frame structural analysis (FRAME) software, that additional rotational fixity at plates significantly contributed to overall structural performance of the truss studied. Cramer et al. [17] presented a metal plate connected wood splice joint and developed a finite element model for tensile and bending analysis by considering nonlinearity, effects of gaps and metal buckling effects, discovering that the bending test results on splice joints were in good agreement with the analytical results. Riley et al. [18] found the maximum vertical deflection and maximum bending moment of the truss members made of fictitious members ranged the values between the pinned and rigid joint models. Vatovec et al. [19] developed a complex finite element model to analyze the metal-plate-connected wood joints in trusses, and concluded that the model response of the tension splice joints depended largely on the stiffness properties of the wood-to-plate interaction elements and the bending joint models were highly depended on the wood-to-wood contact. To validate the results of the analytical joint model, 33 metal-plate-connected joints were tested by Riley [20], who found that the results from the analysis were compared against those from pinned rigid joints. The maximum vertical deflection of truss with semirigid joints fell between the values of pinned and rigid joints. To investigate the behavior of metal plate connected wood truss joints surrounding the open area of attic type trusses under the action of dead and live loads, Kathleen et al. [21] tested the full-scale trusses and conducted the analytical simulation studies involving predictive stiffness models of the metal plate connections. Their results suggested that modeling the joints of metal plate connected wood trusses with nontriangulated openings as partially rigid was necessary for estimating the overall maximum deflection.

Research on the mechanical behavior of structural components made of poplar LVL is very limited. Liu et al. [22] examined the flexural performance of Poplar LVL beam. No publications were found on the structural behavior of poplar LVL trusses. In order to explore the feasibility of poplar LVL light trusses in construction of roof systems, four types of light trusses were designed and manufactured, which were made of poplar LVL and connected with bolts and tooth plates. The trusses were statically tested and analytically modelled in terms of bearing capacity, ultimate load, and deflection character. The failure morphology of each truss was also observed and described.

2 Methods

2.1 Materials and Specimens

2.1.1 Poplar LVL

The poplar LVL used was purchased from Jiangsu Jiuhe Timber Company, which had cross-sectional sizes of 40 mm × 90 mm and density of 0.57 g/cm^3. The poplar LVL met the requirements stipulated in the following standards/codes: General Requirements for Physical and Mechanical Tests of Wood (GB1928-2009) [23], Standard for Test Methods of Timber Structures (GB/T 50329-2012) [24], Standard Test Methods of Static Tests of Lumber in Structural Sizes (ASTM D143-14) [25], and Technical Code for Light Wood Trusses (JGJ/T265-2012) [26]. The physical and mechanical properties of the poplar LVL are given in Tab. 1 [27].

Table 1: Material properties of poplar LVL

Modulus of elasticity (MPa)	The moisture content (%)	Shear strength perpendicular to Grain (MPa)	Compression strength Parallel to Grain (MPa)	Compression strength Perpendicular to Grain (MPa)	Tensile strength parallel to grain (MPa)
9720	12.8	5.6	27.5	3.8	39.4

2.1.2 Truss Selection

The types of light truss specimens were selected and are shown in Tab. 2. In order to study the influence of joint type on the bearing capacity of the trusses, two types of connection were designed, namely bolt connection and tooth plate connection. The details of each truss are shown in Figs. 1–4.

Table 2: Poplar LVL light truss specimens

Specimen code	Truss type	Truss span (m)	Joint connection type
DC-HJ1	Howe	4.5	Bolt connection*
DC-HJ2	Howe	4.5	Tooth plate connection
DC-HJ3	Fink	4.5	Bolt connection*
DC-HJ4	Fink	4.5	Tooth plate connection

*The bolts used were the type of class 8.8 with a diameter of 14 mm and the joint plate used had a thickness of 3 mm.

2.1.3 Tooth Plates

The model of the tooth plate was TR-1, which is made of Q235 carbon steel. Two sizes of tooth plates, 75 mm × 114 mm and 75 mm × 200 mm, were used. The design strength and the shear strength of tooth plates are shown in Tabs. 3 and 4, which are indicated in the Standard for Design of Timber Structures (GB50005-2017) [28].

2.2 Testing

A self-balanced testing device was used for applying load, in which the concentrated load was applied at the upper chord nodes by twisting the bolt of the flower baskets, as shown in Fig. 5. Each truss was equipped with 10 dial indicators and 26 strain gauges. The strain gauges were arranged symmetrically on the upper and lower (or right and left) surfaces of the mid-span section of a truss specimen. The arrangement of the measuring positions is shown in Figs. 6 and 7.

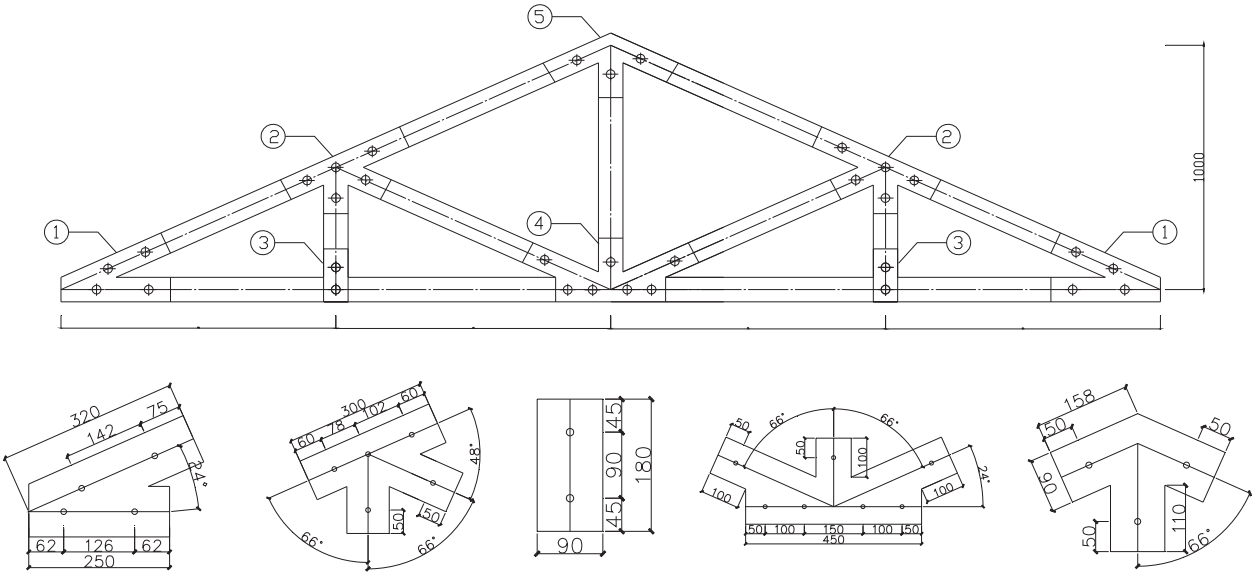

Figure 1: DC-HJ1 and size of joint plate

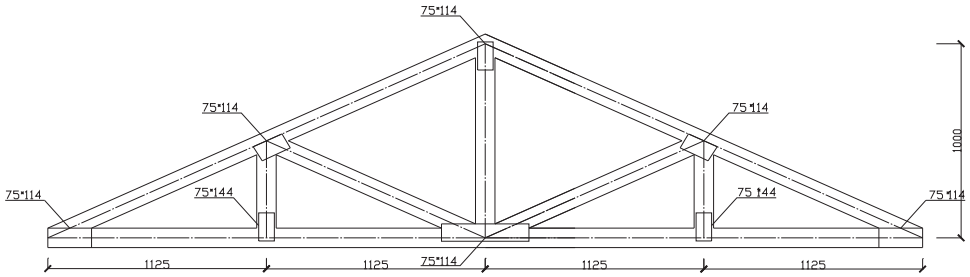

Figure 2: DC-HJ2

2.3 Design Load of the Trusses

According to the Technical Code for Light Wood Trusses (JGJ/T 265-2012) [26], the bearing, tensile and shearing capacities of the plate tooth were calculated respectively, and the minimum value was adopted as the design load, which was 1.2 kN.

The ultimate bearing capacity of the bolt connection between the wood and the steel was 9.6 kN, according to the Standard for Design of Timber Structures (GB 50005-2017) [28], which is the minimum value of bearing and bending strength for pin connection.

2.4 Loading Scheme

The experiment was conducted in the Static Laboratory of the Civil Engineering School, Yangzhou University. Each test was carried out by loading at various stages, with 1/6 design load as the loading step. Before the test, bolts, screws and pressure sensors with holes in the middle were connected, and loads were applied by twisting the basket bolts. The loading values were controlled by the pressure sensors.

The truss test was carried out following the instructions [24], and the loading procedure was divided into three stages: preloading, standard loading and destructive loading, as shown in Fig. 8.

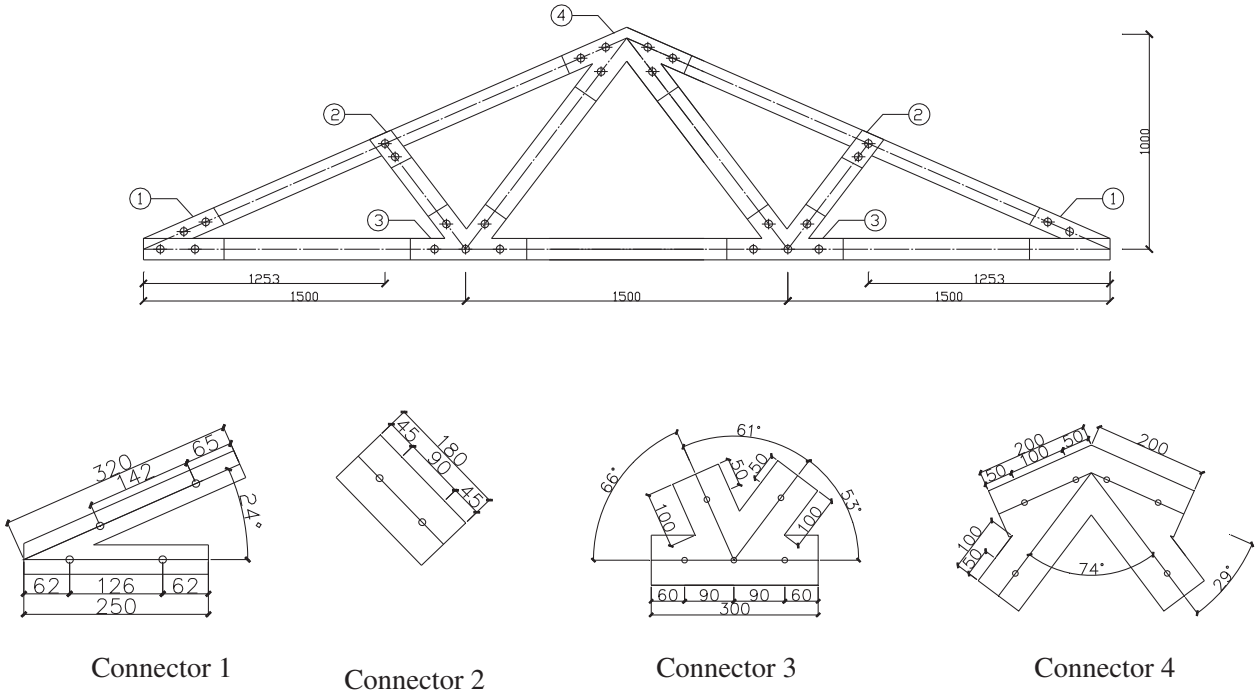

Figure 3: DC-HJ3 and size of joint plate

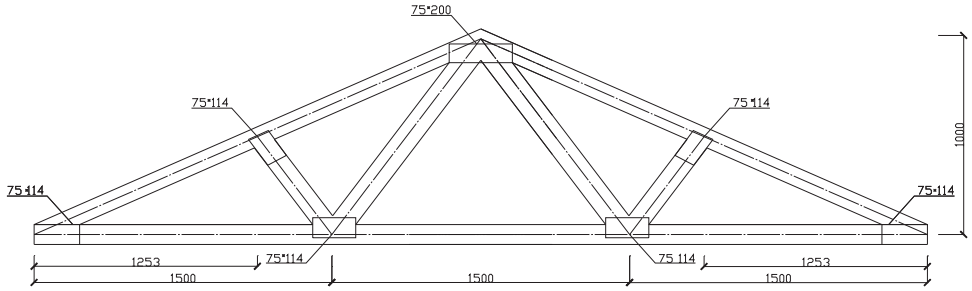

Figure 4: DC-HJ4 and size of tooth plate

Table 3: Design strength of tooth plates

Number	Angle (°)	design strength (N/mm^2)
1	a = 0°, θ = 0°	1.222
2	a = 0°, θ = 90°	2.066
3	a = 90°, θ = 0°	1.085
4	a = 90°, θ = 90°	1.449

A poplar LVL light truss was considered to be destroyed under one of the following conditions:

1. Any member or joint of the truss lose its bearing capacity;
2. The deflection of the truss increased sharply; and

Table 4: Shear strength of tooth plates (N/mm^2)

0°	30°	60°	90°	120°	150°
$v_0 = 85.39$	$v_{30C} = 84.11$	$v_{60C} = 91.7$	$v_{90} = 105.51$	$v_{120C} = 74.97$	$v_{150C} = 88.23$
	$v_{30T} = 115.93$	$v_{60T} = 146.1$		$v_{120T} = 89.18$	$v_{150T} = 114.93$

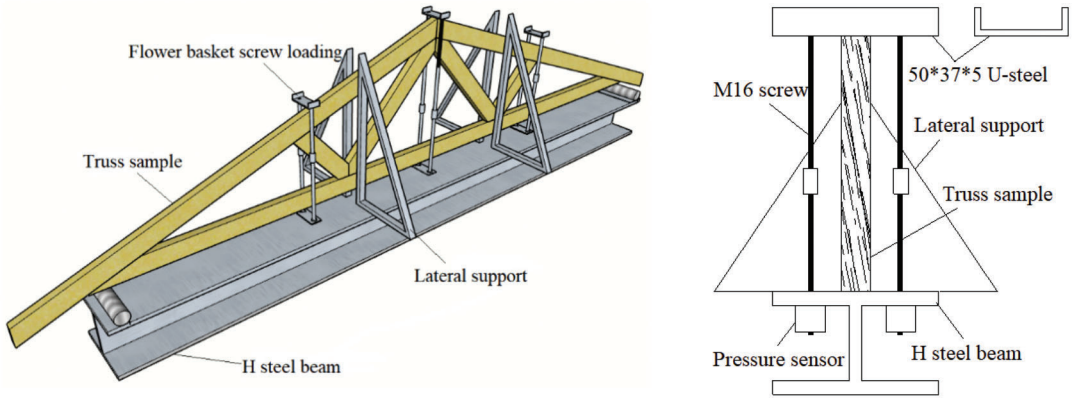

Figure 5: Testing device. (a) Schematic of loading device. (b) Side view of loading device

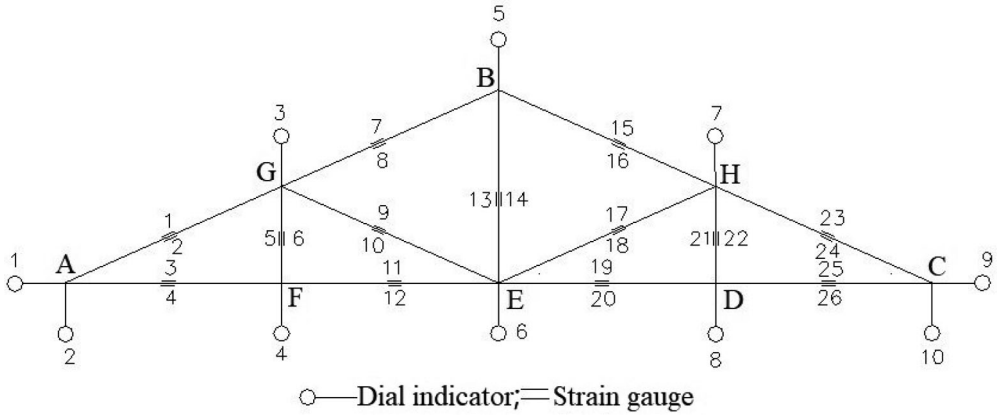

Figure 6: Arrangement of measuring locations for the truss specimens DC-HJ1 and DC-HJ2

3. Any wood splitting occurs at any joint of the truss, or the deformation of the connection exceeded the stipulation of the Standards/Codes.

3 Results and Discussion

3.1 Failure Morphology

3.1.1 Failure Morphology after Stepped Loading and Unloading

Before the load reached the design value, the truss was still in its elastic stage. After unloading to zero for 0.5 h, the residual deformation of each point was measured.

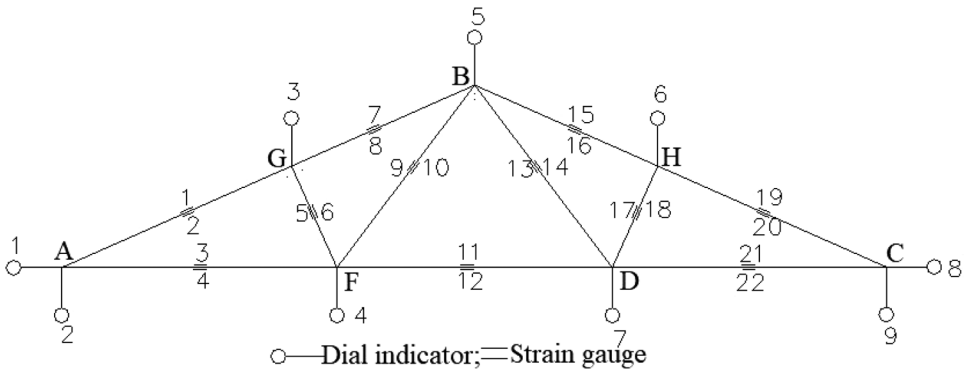

Figure 7: Arrangement of measuring locations for the truss specimens DC-HJ3 and DC-HJ4

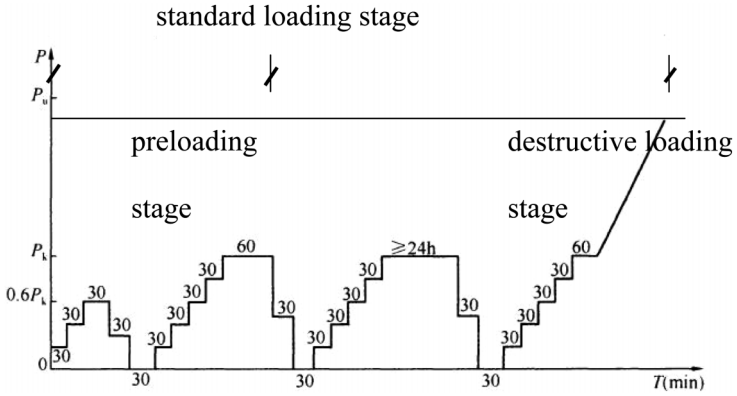

Figure 8: Loading scheme

3.1.2 Failure Morphology after Reloading

When the truss was reloaded to the design load, there was still no damage observed.

During the process in which a truss specimen was loaded to failure, it was found that there was no obvious sign before the failure happened, i.e., the failure was sudden and brittle to some extent. The detailed failure phenomena of each truss specimen are provided in Tab. 5, the final damage pictures are shown in Fig. 9. Among which, the truss specimens DC-HJ1 and DC-HJ3 were suddenly destroyed due to instability of the upper chord, while the specimens DC-HJ2 and DC-HJ4 were destroyed due to the ultimate bearing capacity of the heel joints.

3.2 Testing Results

The ultimate load and joint deflection of the truss specimens are shown in Tab. 6. Here the deflection at each measuring location was calculated by subtracting the settlement of the support from the deflection value.

As shown in Tab. 6, the ultimate loads of the four specimens tested are 16.6 kN, 7.4 kN, 18.2 kN and 11.4 kN, which are 6–15 times as large as the design values. For the trusses of the same type and the same test span, the bearing capacity of the trusses with bolted connections is larger than that with tooth plate connections. This could be attributed to the stronger restraints of the joints provided by the bolted connections compared with that by the plate tooth ones. When the trusses had the same span, it was found that the bearing capacity of the Fink trusses was greater than that of the Howe trusses.

Table 5: Failure morphology of the poplar LVL trusses tested

Specimen Code	Load (kN)	Failure morphology
DC-HJ1	0–14.6	No damage happens was observed.
	14.8	The upper chord of the truss began to deflect and deform with slight cracking.
	16.6	The chord deformation of the truss was obvious and the truss was damaged.
DC-HJ2	0–6.2	No damage happened.
	6.4	The trusses began to rattle slightly, and the member at the supports began to deform.
	7.4	The tooth plate at the support was bent, and was pulled out from the member. The member at the joint was torn and damaged.
DC-HJ3	0–15.8	No damage happened.
	16.0	The upper chord of the truss began to buckle and deform with slight cracking.
	18.2	The chord deformation of the truss was obvious and the truss was damaged.
DC-HJ4	0–9.0	No damage happened.
	9.2	There was cracking in the truss and a 3-mm-crack was found at the truss support.
	10.8	The crack extended to 7 mm in width with continuous cracking, and the surface of the truss chord emerged with wrinkles and bulged.
	11.2	With crackling continuing, wrinkles and bulges became more pronounced.
	11.4	The tooth plate at the support was bent, and was pulled out from the LVL member. The member at the joint was torn and damaged.

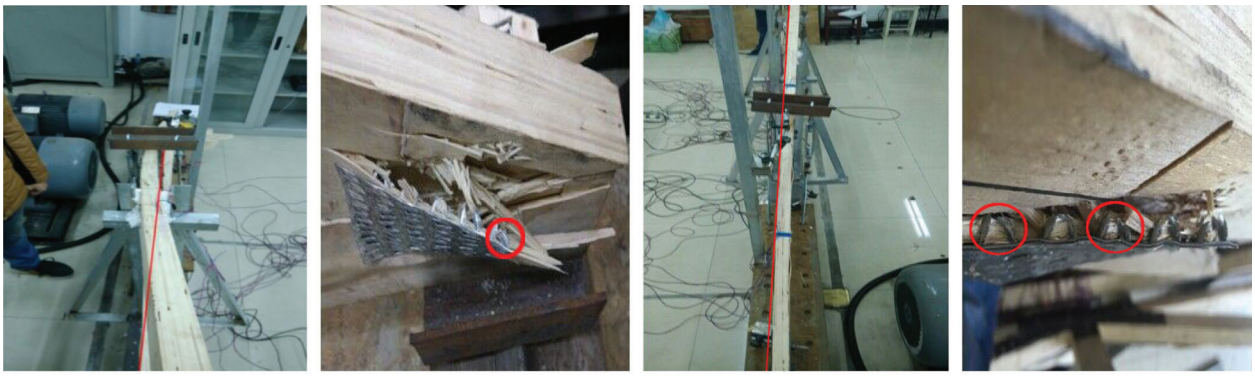

(a) (b) (c) (d)

Figure 9: Failure morphology of the trusses. (a) DC-HJ1, (b) DC-HJ2, (c) DC-HJ3, (d) DC-HJ4

Tab. 7 compares, in terms of the ratio of strength (ultimate loading capacity) to weight and the unit ultimate bearing capacity, the poplar LVL trusses fabricated and tested in this study with the light trusses reported by Xu [10]. It can be found that the poplar LVL trusses exhibited a better mechanical performance than the light trusses. It should be indicated that the configurations of two types of poplar LVL trusses were the same as those used by Xu [10], except using the different materials and connections. Xu [10] used dimension spruce-pine-fir lumber of a grade of #2 and better, and truss plates. The authors employed poplar LVL and truss plates/bolts for making connections. The poplar LVL has

Table 6: The testing results of the truss specimens tested

Content		Specimen			
		DC-HJ1	DC-HJ2	DC-HJ3	DC-HJ4
Ultimate load P (kN)		16.60	7.40	18.20	11.40
F*-point deflection (mm)	Design load	0.90	0.57	1.19	0.78
	Ultimate load	19.35	6.86	19.33	13.67
	Maximum displacement	19.98	7.52	20.06	14.48
G-point deflection (mm)	Design load	0.84	0.68	1.13	0.89
	Ultimate load	19.46	7.21	19.24	9.16
	Maximum displacement	19.71	7.30	19.51	9.35
E-point deflection (mm)	Design load	1.36	0.81		

*See Figs. 6 and 7.

Table 7: Comparison of the strength-weight ratio and unit ultimate bearing capacity between this study and the [10]

Specimen number	Strength-weight ratio ($kN/(g/cm^3)$)		Unit ultimate bearing capacity (kN/m)	
	This study	[10]	This study	[10]
1	29.12	3.03	3.69	0.21
2	12.98	3.50	1.64	0.25
3	31.93	3.73	4.04	0.26
4	20.00	3.03	2.53	0.21
Mean	23.51	3.32	2.98	0.23

more uniform anatomical structure in materials (e.g., without knots) than sawn lumber and acceptable mechanical properties, therefore, the trusses made of poplar LVL could show a better structural performance.

3.3 Relationship between the Load and the Deflection of the Lower Chord Joints

The load-deflection curves for joints F, E and D of each truss specimen are illustrated in Fig. 10. It can be found that the initial stiffness of Specimen DC-HJ1 is slightly higher than that of Specimen DC-HJ2, while the initial stiffness of Specimen DC-HJ3 is almost the same as that of Specimen DC-HJ4. The bearing capacity and the deflection of the trusses with bolted connections are larger than those of the trusses with tooth plate connections. In the early stage of loading, the load-deflection curve of each truss shows a good linear relationship. In the later stage of loading, the bending rigidity of each truss decreases with the fast increasing deflection. As for failure, neither of the trusses shows excessive plastic deformations.

3.4 Relationship between the Load and the Axial Strain of the Upper Chord of the Truss

Fig. 11 shows the load-strain curves of the upper chord members of the trusses, where the strain of each member is the average value of the strains from two measuring locations. As shown in Fig. 10, the load-strain curve of each truss is basically linear up to the design value, and the upper chord of the truss is basically within its elastic stage. When the load is added up to twice the design value, the individual upper chord

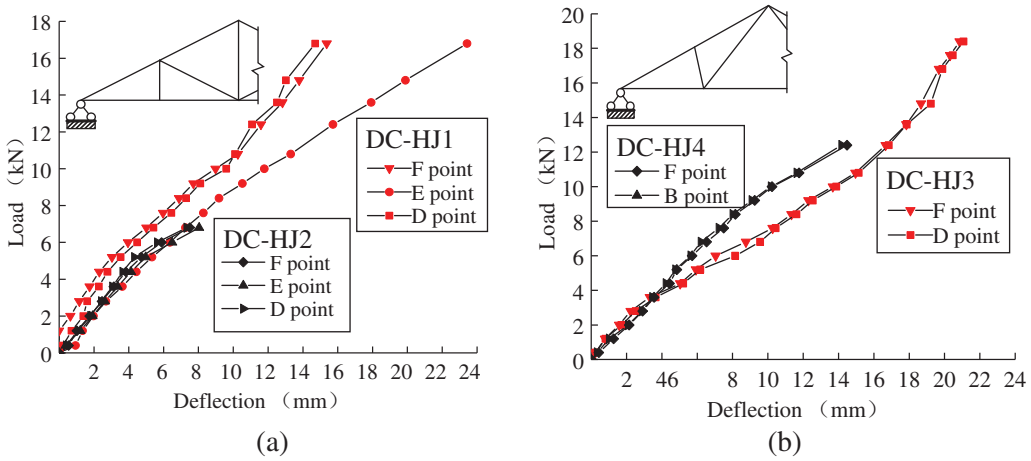

Figure 10: Load-deflection curves for the lower chord joints. (a) DC-HJ1 and DC-HJ2. (b) DC-HJ3 and DC-HJ4

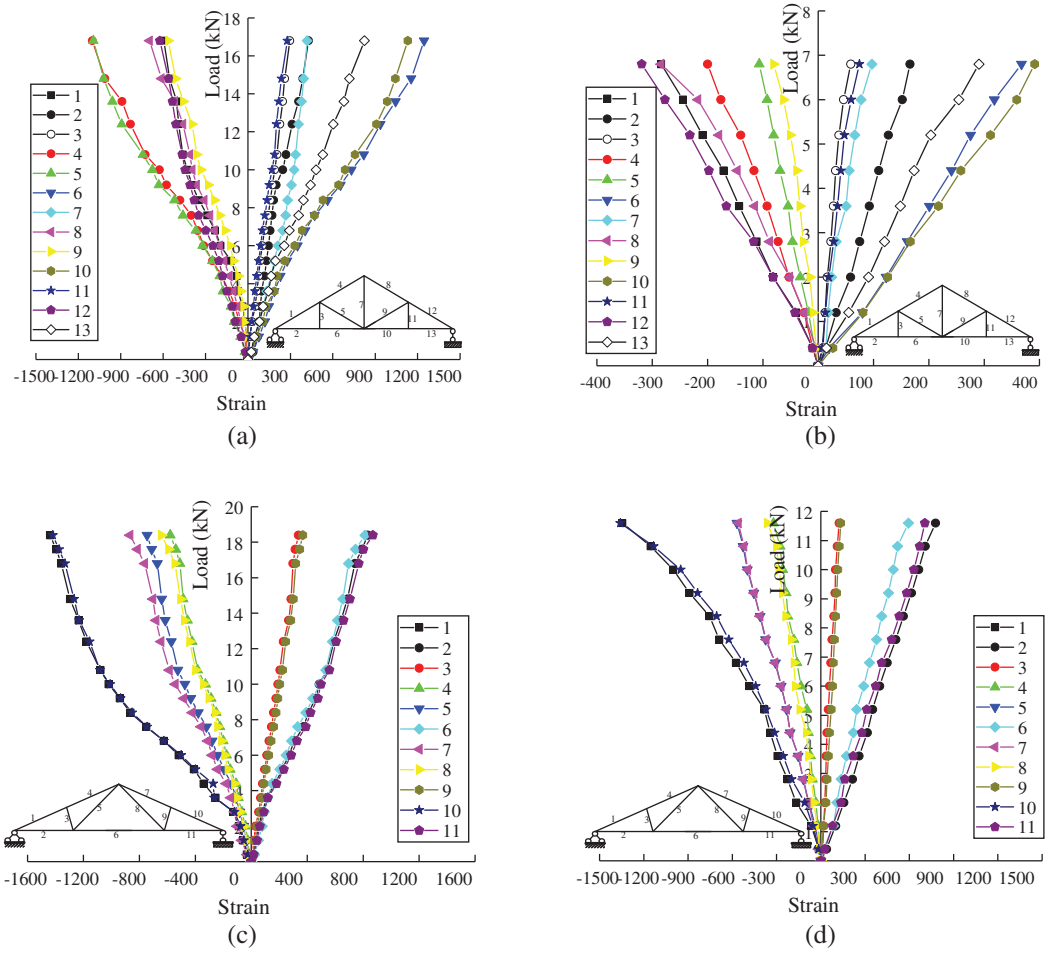

Figure 11: Axial load-strain curves of the truss specimens tested. (a) DC-HJ1. (b) DC-HJ2. (c) DC-HJ3. (d) DC-HJ4

of the bolt-connected truss begins to show some non-linear properties, and the slope of the load-strain curve begins to increase, indicating that the upper chord of the trusses enters elastic-plastic stage. Until the truss is loaded to failure, there is no obvious plastic change in the members of each truss specimen.

4 Analysis and Modelling

In the case of the effects of self weight, joint eccentricity and joint rigidity can be neglected, a truss can be modelled as the pin-jointed system under the action of concentrated joint load. However, when those conditions, such as rigid joint, semi-rigid joint or joint zone, cannot be met, a more sophisticated model shall be employed,

To simulate the semi-rigid joint, four main types of equations can be adopted, i.e., models using spring elements, with fictitious elements, with small fictitious beams of reduced elasticity modulus, and with special elements that describe the behavior of a joint [29]. In this study, the analytical model with spring elements is developed to consider the semi-rigid nature of the truss joint. Based on the study by Gupta et al. [30], the axial stiffness can be, by considering the difference in materials, expressed as:

$$k_{\mathrm{A}} = 0.13EA/L \quad \text{for heel joint with bolt connection} \tag{1}$$

$$k_{\mathrm{A}} = 0.05EA/L \quad \text{for heel joint with tooth plate connection} \tag{2}$$

$$k_{\mathrm{A}} = 0.20EA/L \quad \text{for web joint with bolt connection} \tag{3}$$

$$k_{\mathrm{A}} = 0.11EA/L \quad \text{for web joint with tooth plate connection} \tag{4}$$

Considering the fact that the rotational stiffness has little effect on the result of axial force under the action of joint load, the joints are assumed to be rigid along the rotational direction. As a standard analysis method stipulated in the Chinese code [28], the continuous member at the joint is modelled as rigid connected one, while the web member at the joint is modelled as pin connected one. Specially, the heel joint of a truss is modelled as a joint zone, which consists of three sub-joints and three sub-members, as shown in Fig. 12.

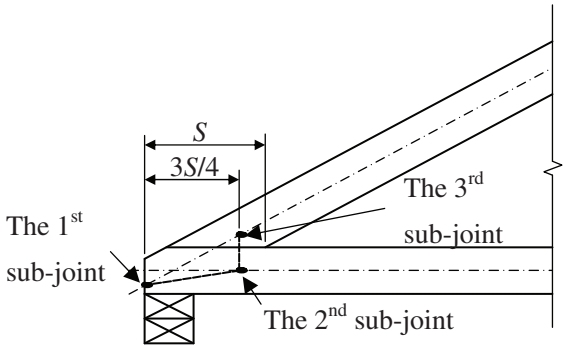

Figure 12: The heel joint zone modelling based on the Chinese code [27]

Thus, four kinds of modelling are established and compared in this study, namely truss with pin joints, truss with rigid joins, truss with spring elements and truss proposed in the Chinese codes [25,27].

5 Discussion on the Load Carrying Capacity of the Trusses

The experimental results show that, for the bolt-connected truss specimens (DC-HJ1 and DC-HJ3), the failure was controlled by the out-of-plane instability of the top chord members, while for the tooth-plate-connected truss specimens (DC-HJ2 and DC-HJ4), the failure was due to damage of the heel joints.

Under the action of joint load, the top chord member can be regarded as axially loaded compressive column, and the capacity can be expressed as stipulated in the Chinese code [31]:

$$N = \varphi f_c A \tag{5}$$

where, A is the area of the section, f_c is the adjusted compressive design strength parallel to grain, and φ is the stability factor which can be calculated by the following formulas [31]:

$$\varphi = \frac{1 + (f_{cE}/f_c)}{1.8} - \sqrt{\left[\frac{1 + (f_{cE}/f_c)}{1.8}\right]^2 - \frac{f_{cE}/f_c}{0.9}} \tag{6}$$

$$f_{cE} = \frac{0.47E}{(l_0/b)^2} \tag{7}$$

$$l_0 = k_l l \tag{8}$$

where, E is the adjusted modulus of elasticity, b is the side length of the section, l is the length of the member, and k_l is the effective length factor. According to the Chinese code [31], f_c and E should be adjusted under the following cases: the moisture content of a member exceeds 15%; the surface temperature of the member reaches 40°C to 50°C due to long-term surrounding high temperature; the load combination is dominated by dead load. In the study, the moisture content is 12.8%, the temperature is no more than 38°C, and apparently the load is a kind of short-term load, so f_c and E are not required to be adjusted. The values of compressive strength and modulus of elasticity in the parallel to grain direction are taken as 27.5 MPa and 9,720 MPa, respectively, according to Tab. 2. Considering the lateral steel support for the top chord member, the member length l should be taken as the distance between the lateral support and the heel joint. As for the effective length factor k_l, it should be notice that the lateral support cannot restrain the member rotation in the out of plane. On the other hand, the heel joint can, compared to the lateral support, do it to a certain extent, which can be verified by the experimental results. As a result, it can be reasonably assumed that the instability mode is hinge at the support and fixed at the heel joint, i.e., k_l can be set to 0.8 [31].

Based on the observation of testing, the damage of the heel joint with tooth plate connection could be divided into two stages. In the first stage, there was almost no sliding between the tooth plate and the poplar LVL member, since the load was borne by the plate tooth and the anti-sliding bearing capacity of the tooth plate. In the second stage, the member surface began to crack, the plate teeth were gradually pulled out from the poplar LVL members. Finally the tooth plate was bent and the member at the joint was torn. In this stage the load was borne by the shear-tension bearing capacity of the tooth plate. Following the Chinese standard [28], the anti-sliding bearing capacity N_S and the shear-tension bearing capacity C_r for the 75 mm × 114 mm tooth plate at the heel joint can be calculated, which are 7.18 kN and 12.81 kN, respectively, for the bottom chord, compared to 5.74 kN and 11.93 kN for the top chord. It should be noticed that the joint damage of Specimen DC-HJ2 occurred at the top chord, while the damage of Specimen DC-HJ4 appeared at the bottom chord.

Based on the above discussion, the ultimate load, the load at which damage began, and the bearing capacity of those calculated from the four types of joint modelling for the bolt-connected trusses (DC-HJ1 and DC-HJ3) are compared in Fig. 13, and the deflection under the above cases is shown in Fig. 14. From these two figures, it can be concluded that the calculating results from the spring model are very close to those from tests at which the damage began, while the results from other three models are almost the same under the action of concentrated joint load, which are not so good as that of the spring model.

As for the tooth-plate-connected trusses, the situation is much more complex. Figs. 15 and 16 show the ultimate load from the experiment, the load at which damage began, and the bearing capacity of those

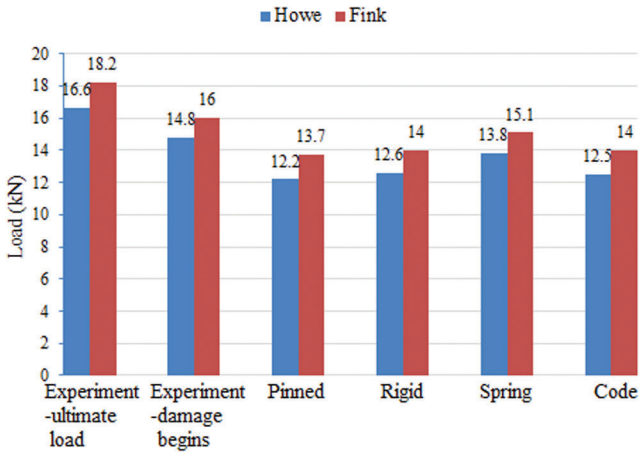

Figure 13: Comparison of bearing capacity between the bolt-connected Howe and Fink trusses

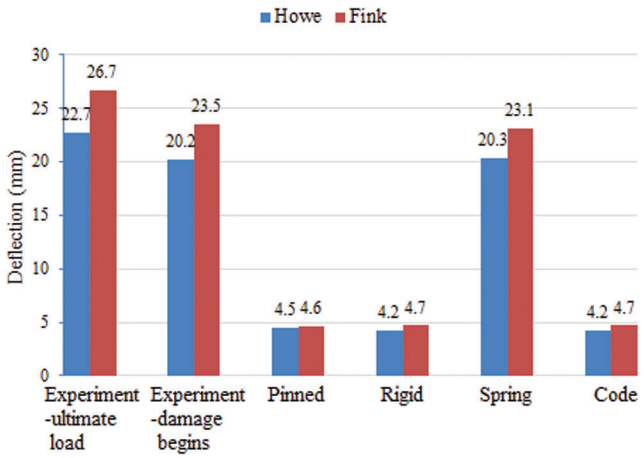

Figure 14: Comparison of deflection between the bolt-connected Howe and Fink trusses

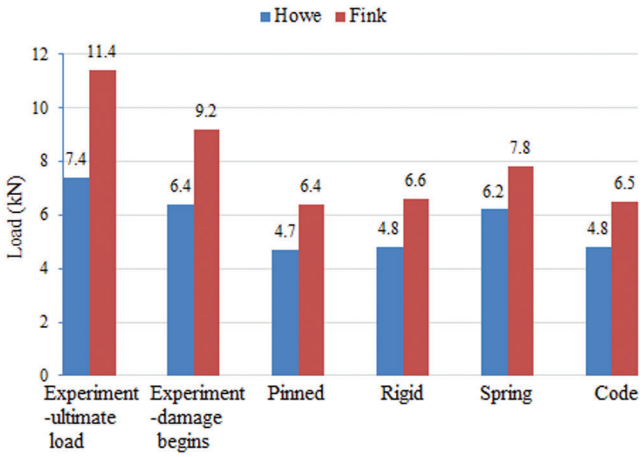

Figure 15: Comparison of bearing capacity between the tooth-plate-connected trusses in terms of the anti-sliding bearing capacity *N*s

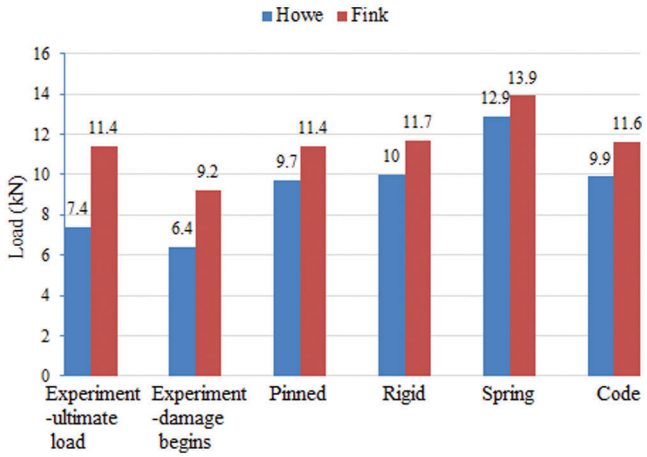

Figure 16: Comparison of bearing capacity between the tooth-plate-connected trusses in terms of the shear-tension bearing capacity *C*r

calculated from the four types of joint modelling for the tooth-plate-connected trusses (DC-HJ2 and DC-HJ4) based on N_S and C_r, the corresponding deflections are shown in Figs. 17 and 18. It can be found that the results calculated from the spring model are reasonably, when N_S is used, close to the testing results when damage began. Use of C_r makes other three models more reasonable to explain for the ultimate load capacity, especially for Specimen DC-HJ4. As for the deflection, neither of the four models can well describe the experimental results, among which when N_S is used, the results from the spring model are in better agreement with the experimental results in terms of the ultimate load.

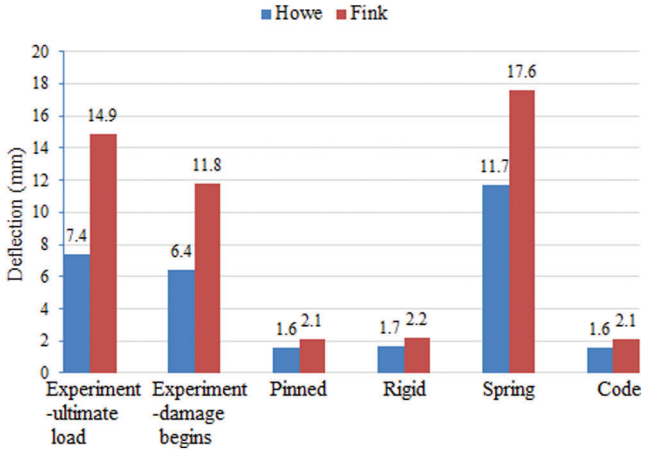

Figure 17: Comparison of deflection between the tooth-plate-connected trusses in terms of the anti-sliding bearing capacity *N*s

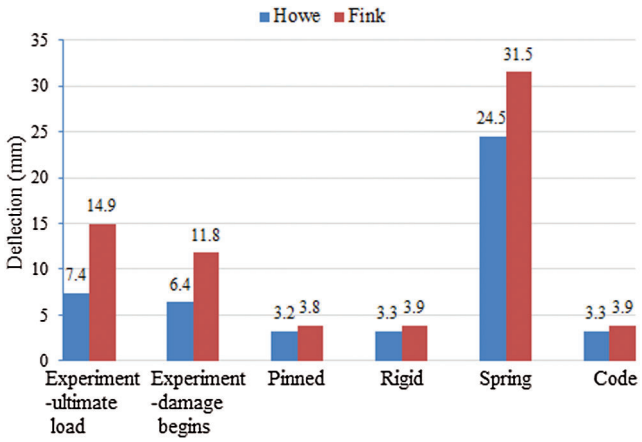

Figure 18: Comparison of deflection between the tooth-plate-connected trusses in terms of the shear-tension bearing capacity *C*r

6 Conclusions

To promote the use of poplar LVL light trusses in roof construction, both experimental testing and theoretical analysis were conducted on two kinds (i.e., Howe and Fink) of classical light trusses connected with bolts and tooth plates. The testing results showed that the poplar LVL light trusses had a satisfactory performance that could meet the required design values stipulated in Chinese standards and codes. The spring model could well predict the experimental results. The main conclusions from this study could be drawn as follows:

1. The poplar LVL light trusses basically behaved in the elastic stage when the load applied was up to the design value.
2. The bearing capacity of the Fink trusses was greater than that of the Howe trusses.
3. The testing results showed that the failure of the bolt-connected trusses was mainly due to instability of the upper chord, while the failure of the tooth-plate-connected trusses was mainly due to the ultimate bearing capacity of the heel joints. Thus, in structural design, the length of the upper chord should be paid attention to the bolt-connected trusses, while the strengthening of the heel joints should be considered for the tooth-plate-connected ones.
4. As for the bolt-connected trusses, the spring model showed a good agreement, in terms of either load or deflection, with the experiment results at the start of damage. As for the tooth-plate-connected trusses, the spring model could reasonably, when the anti-sliding bearing capacity *N*s was used, estimate the load capacity at the initiation of damage at heel joints.

In summary, the poplar LVL light trusses with either bolted- or truss-plated connection showed a great potential in construction such as the roof system of a building.

Acknowledgement: The authors would like to express sincere thanks to Ministry of Science and Technology and Housing and Urban-Rural Development of China.

Funding Statement: This research was funded by National Key Research and Development Plan "Green Building and Building Industrialization" Key Special Project in 2017 (Grant No. 2017YFC0703505) and Ministry of Housing and Urban-Rural Development Technology Project in 2015 (Grant No. 2015-K2-009).

Conflicts of Interest: The authors declare that they have no conflicts of interest to report regarding the present study.

References

1. Hong, C. K., Li, H. T., Lorenzo, R., Wu, G., Corbi, I. et al. (2019). Review on connections for original bamboo structures. *Journal of Renewable Materials, 7(8),* 713–730. DOI 10.32604/jrm.2019.07647.
2. Li, H. T., Qiu, Z. Y., Wu, W., Wei, D. W., Lorenzo, R. et al. (2019). Compression behaviors of parallel bamboo strand lumber under static loading. *Journal of Renewable Materials, 7(7),* 583–600. DOI 10.32604/jrm.2019.07592.
3. Zhang, H. Y., He, Q., Lu, X. N., Pizzi, A., Mei, C. T. et al. (2018). Energy release rate measurement of welded bamboo joints. *Journal of Renewable Materials, 6(1),* 450–456. DOI 10.7569/JRM.2017.634154.
4. Xu, X. L., Ma, R. L., He, M. J. (2006). Analysis of light wood truss test and bearing capacity. *Special Structures, 23 (1),* 1–4 (in Chinese).
5. Yang, Y., Xie, Y. B., Fei, B. H., Wang, X. H., Sun, Y. G. (2013). Comparative study of mechanical properties of the three wood metal-plate connection. *Wood Processing Machinery, 24(3),* 17–21 (in Chinese).
6. Pratiwi, N., Tjondro, J. A. (2018). Study on strength and stiffness of meranti wood truss with plywood gusset plate connection and lag screw fastener. *Journal of the Civil Engineering Forum, 4(1),* 51–66. DOI 10.22146/jcef.30230.
7. Sagara, A., Tjondro, J. A., Shiddiq, H. A. (2017). Experimental study on strength and stiffness connection of wooden truss structure. *MATEC Web of Conferences, 101,* 01015. DOI 10.1051/matecconf/201710101015.
8. Xiao, Y., Chen, G., Feng, L. (2014). Experimental studies on roof trusses made of glubam. *Materials and Structures, 47(11),* 1879–1890. DOI 10.1617/s11527-013-0157-7.
9. Matteo, B., Alberto, C., Lorenzo, F., Massimo, M., Marco, T. (2014). Innovative connection in wooden trusses. *Construction and Building Materials, 66,* 654–663. DOI 10.1016/j.conbuildmat.2014.06.022.
10. Xu, X. L. (2006). *Research on bearing capacity of light wood truss*. Shanghai: College of Civil Engineering, Tongji University (in Chinese).
11. Beineke, L. A., Suddarth, S. K. (1979). Modeling joints made with light-gage metal connector plates. *Forest Products Journal, 42(3),* 761–770.
12. Misra, R. D. (1964). *An analytical and experimental investigation of stress distribution in the punched metal plate of a timber joint (Ph.D. Thesis)*, Michigan State University, Ann Arbor, MI, USA.
13. Foschi, R. O. (1979). Truss plate modeling in the analysis of trusses. *Proceedings of Metal Plate Wood Truss Conference*. Madison, WI, USA: Forest Products Research Society.
14. Toan, V. D. (1980). *Behavior of metal plate connection in wood trusses (MS Thesis),* University of California, Davis, CA, USA.
15. Maraghechi, K., Itani, R. Y. (1984). Influence of truss plate connectors on the analysis of light frame structures. *Wood and Fiber, 16(3),* 306–322.
16. Lum, C., Varoglu, E. (1988). Testing and analysis of parallel chord trusses. In Seattle, R. Y. I. (ed.), *Proceedings of the International Conference on Timber Engineering,* vol. 1. Madison, WI, USA: PForest Products Research Society.
17. Cramer, S. M., Shrestha, D., Mtenga, P. V. (1993). Computation of member forces in metal plate connected wood trusses. *Structural Engineering Review, 5(3),* 209–217.
18. Riley, G. J., Gebremedhin, K. G., White, R. N. (1993). Semi-rigid analysis of a metal plate connected wood truss using fictitious members. *Transactions of the ASAE, 36(3),* 887–894. DOI 10.13031/2013.28413.
19. Vatovec, M., Miller, T. H., Gupta, R., Lewis, S. (1997). Modeling of metal-plate-connected wood truss joints: part II—truss behavior. *Transactions of the ASAE, 40(6),* 1667–1675. DOI 10.13031/2013.21411.
20. Riley, G. J. (1998). Analytical model of metal-plate-connected wood truss joint stiffness (Ph.D. Thesis), Cornell University, Ithaca, NY, USA.
21. Rittenburg, K. A. W., Kunnath, S. K. (2003). Deflection of metal plate connected wood trusses with nontriangulated openings. *Journal of Structural Engineering, 129(11),* 1546–1558. DOI 10.1061/(ASCE)0733-9445(2003)129:11(1546).

22. Liu, W. Q., Yang, H. F. (2008). Experimental study on flexural behavior of engineered wood beams. *Journal of Building Structures, 29(1),* 90–95, (in Chinese).
23. GB1927-2009. (2009). *General requirements for physical and mechanical tests of wood*. Beijing: China National Standardization Administration (in Chinese).
24. GB/T 50329-2012. (2012). *Standard for test methods of timber structures*. Beijing: China National Standardization Administration (in Chinese).
25. ASTM. (2019). *Standard test methods of static tests of lumber in structural sizes. Designation: D143-09*. West Conshohocken, PA: ASTM International.
26. JGJ/T. (2012). *Technical code for light wood trusses. Designation: JGJ/T 265*. Beijing: China National Standardization Administration (in Chinese).
27. Liu, Y., Wang, H. H., Ding, P. R., Song, Y. L. (2017). The physical and mechanical properties of the poplar LVL. *China Forest Products Industry, 44(2),* 12–16 (in Chinese).
28. GB. (2017). *Standard for design of timber structures. Designation: GB 50005*. Beijing: China National Standardization Administration (in Chinese).
29. Ellegaard, P. (2006). Finite-element modeling of timber joints with punched metal plate fasteners. *Journal of Structural Engineering, 132(3),* 409–417. DOI 10.1061/(ASCE)0733-9445(2006)132:3(409).
30. Gupta, R., Gebremedhin, K. G. (1990). Destructive testing of metal plate connected wood truss joints. *Journal of Structural Engineering, 116(7),* 1971–1982. DOI 10.1061/(ASCE)0733-9445(1990)116:7(1971).
31. GB. (2012). *Technical code of glued laminated timber structures. Designation: GB/T 50708*. Beijing: China National Standardization Administration (in Chinese).